Defence Research and Development Canada
Recherche et développement pour la défense Canada

DEFENCE DÉFENSE

Initial results of HF sky wave radar experiments using MIMO methods to control auroral clutter

R. J. Riddolls

Defence R&D Canada – Ottawa

Canada

Technical Memorandum
DRDC Ottawa TM 2009-268
January 2010

Initial results of HF sky wave radar experiments using MIMO methods to control auroral clutter

R. J. Riddolls
Defence R&D Canada – Ottawa

Defence R&D Canada – Ottawa
Technical Memorandum
DRDC Ottawa TM 2009-268
January 2010

Principal Author

Original signed by R. J. Riddolls

R. J. Riddolls

Approved by

Original signed by D. Dyck

D. Dyck
Head/Radar Systems Section

Approved for release by

Original signed by B. Eatock

B. Eatock
Head/Document Review Panel

Abstract

High frequency Over-the-Horizon Radar (OTHR) provides an economical means to track noncooperative air targets over large expanses of land and ocean. However, early attempts to run OTHR in Canada in the 1970s were confounded by the presence of intense radar clutter originating in the auroral zone. Recent advances in Multiple-Input Multiple-Output (MIMO) OTHR technology, namely orthogonal waveform transmit arrays and fully sampled receive arrays, provide an opportunity to revisit the possibility of OTHR in Canada. An OTHR testbed has been built in Ottawa, Canada to determine the capabilities of the technology. The testbed consists of a MIMO OTHR with 4 transmit channels and 4 receive channels. Some preliminary data show that MIMO processing is effective in cancelling the clutter. It is then proposed to upgrade the testbed to a larger-scale system.

Résumé

Un radar transhorizon (OTHR) à haute fréquence (HF) est un moyen économique de suivre des cibles aériennes non coopératives sur de grandes étendues de terre et de mer. Par contre, dans les années 1970, les premiers essais réalisés au Canada sur un OTHR ont échoué en raison du clutter radar intense qui provient de la zone aurorale. Des innovations récentes dans la technologie des OTHR à entrées et à sorties multiples (MIMO), notamment les réseaux d'émission à forme d'onde orthogonale et les réseaux de réception entièrement échantillonnés, donnent l'occasion de réexaminer l'utilisation possible d'un OTHR au Canada. Un banc d'essai OTHR a donc été construit à Ottawa, au Canada, en vue de déterminer les capacités de la technologie. Ce banc d'essai se compose d'un OTHR MIMO doté de quatre canaux d'émission et de quatre canaux de réception. Selon des données préliminaires, le traitement MIMO permet d'éliminer le clutter. Par conséquent, on suggère d'augmenter la taille du banc d'essai.

This page intentionally left blank.

Executive summary

Initial results of HF sky wave radar experiments using MIMO methods to control auroral clutter

R. J. Riddolls; DRDC Ottawa TM 2009-268; Defence R&D Canada – Ottawa; January 2010.

High frequency Over-the-Horizon Radar (OTHR) provides an economical means to track noncooperative air targets over large expanses of land and ocean. Early attempts to run OTHR in Canada in the 1970s were confounded by the presence of intense radar clutter originating in the auroral zone. In Canada, the auroral zone passes through the center of the country and is hard to avoid in any reasonable OTHR layout for airspace surveillance. However, recent advances in Multiple-Input Multiple-Output (MIMO) OTHR technology, namely orthogonal waveform transmit arrays and fully sampled receive arrays, provide an opportunity to revisit the possibility of OTHR in Canada.

The MIMO OTHR being considered consists of M transmit channels and N receive channels. The M transmit channels each consist of an individual antenna transmitting an orthogonal waveform. The N receive channels each consist of an individual antenna and receiver recording the target echoes of all M transmitted waveforms. The M waveforms are separated in each of the N receivers and an $MN \times 1$ snapshot vector is formed containing all the transmit/receive signal components. Transmit and receive beamforming can be realized by computing linear combinations of the elements of this snapshot vector. Use of a Minimum Variance Distortionless Response (MVDR) beamformer on both transmit and receive leads to an improvement in target signal-to-clutter ratio proportional to the product MN and inversely proportional to the square of $1-\rho$, where ρ is the correlation coefficient of clutter from adjacent channels.

An experimental OTHR testbed has been built in Ottawa, Canada, which contains $M = 4$ transmit channels and $N = 4$ receive channels. The Ottawa OTHR is aimed in the magnetic north direction, toward the earth's auroral zone. Clutter data have been collected during an experimental run with $M = 2$ and $N = 1$. Examination of the data shows that the auroral clutter echoes are consistent with global plasma convection maps deduced by the SuperDARN radar network. Furthermore, a linear combination of the two transmit channels, which effectively places a transmit null in the direction of the clutter, is shown to eliminate the clutter. However, the clutter is only 10 dB above the background noise floor, so it is not clear whether the proposed methods will work for large clutter-to-noise ratios (CNRs).

Finally, it is proposed to increase the power-aperture product of the radar by 20 dB to show the limits of the proposed signal processing strategies at higher CNRs. This

improvement can be realized by a 10-dB increase in the radar transmit power and a 10-dB increase in the receive array aperture. Furthermore, the methods need to be demonstrated against realistic targets, which could be realized by the deployment of a transponder downrange of the radar.

Sommaire

Initial results of HF sky wave radar experiments using MIMO methods to control auroral clutter

R. J. Riddolls; DRDC Ottawa TM 2009-268; R & D pour la défense Canada – Ottawa; janvier 2010.

Un radar transhorizon (OTHR) à haute fréquence (HF) est un moyen économique de suivre des cibles aériennes non coopératives sur de grandes étendues de terre et de mer. Dans les années 1970, les premiers essais réalisés au Canada sur un OTHR ont échoué en raison du clutter radar intense qui provient de la zone aurorale. Au Canada, la zone aurorale traverse le centre du pays et est difficile à éviter pour toute configuration raisonnable de l'OTHR utilisée aux fins de surveillance de l'espace aérien. Par contre, des innovations récentes dans la technologie des OTHR MIMO, notamment les réseaux d'émission à forme d'onde orthogonale et les réseaux de réception entièrement échantillonnés, donnent l'occasion de réexaminer l'utilisation possible d'un OTHR au Canada.

L'OTHR MIMO étudié comporte M canaux d'émission et N canaux de réception. Chacun des M canaux d'émission comprend une antenne individuelle qui émet une forme d'onde orthogonale. Chacun des N canaux de réception comprend une antenne individuelle et un récepteur qui enregistre les échos de cible de toutes les M formes d'onde émises. Les M formes d'onde sont en outre espacées dans chacun des N récepteurs, et un vecteur instantané $MN \times 1$ se forme et contient toutes les composantes du signal d'émission/de réception. On peut calculer les combinaisons linéaires des éléments de ce vecteur instantané pour mettre en forme le faisceau d'émission et de réception. L'utilisation, tant à l'émission qu'à la réception, d'un conformateur de faisceau à réponse sans distorsion à variance minimale (MVDR) a permis d'améliorer le rapport signal/clutter de la cible de façon proportionnelle au produit MN et inversement proportionnelle au carré de $1 - \rho$, où ρ est le coefficient de corrélation du clutter des canaux adjacents.

Un banc d'essai OTHR expérimental a été construit à Ottawa, au Canada, et comporte $M = 4$ canaux d'émission et $N = 4$ canaux de réception. L'OTHR d'Ottawa est orienté vers le nord magnétique, en direction de la zone aurorale de la Terre. Les données sur le clutter ont été recueillies pendant une série d'essais réalisés avec $M = 2$ et $N = 1$. L'examen des données montre que les échos de clutter auroral concordent avec les cartes globales de convection du plasma produites par le réseau radar SuperDARN. De plus, une combinaison linéaire des deux canaux d'émission, qui réussit à donner une valeur nulle à l'émission dans la direction du clutter, permet d'éliminer le clutter. Par contre, comme le clutter est supérieur de seulement 10 dB

au plancher de bruit de fond, on ne peut pas déterminer clairement si les méthodes proposées fonctionneront pour des rapports clutter/bruit (C/B) élevés.

Finalement, on propose d'augmenter de 20 dB le produit puissance-ouverture du radar pour montrer les limites des stratégies de traitement de signal proposées à des rapports C/B plus élevés. Cette amélioration peut être apportée par une augmentation de 10 dB de la puissance d'émission du radar et de 10 dB de l'ouverture du réseau de réception. Par ailleurs, les méthodes doivent être démontrées à l'aide de cibles réelles, qui pourraient être produites par le déploiement d'un émetteur-récepteur en aval du radar.

Table of contents

This page intentionally left blank.

1 Introduction

In 1971 the Rome Air Development Center (RADC) installed the northward-pointing Polar Fox II OTHR in Caribou, Maine, USA, along with transponders in Narssarssuaq and Thule, Greenland, and Keflavik, Iceland [1]. The aim was to determine OTHR performance within the auroral zone. The following year, a collaboration between the US Air Force and the Canadian Defence Research Board led to the installation of the Polar Cap III OTHR in Hall Beach, Northwest Territories, Canada, and a second receive site in Cambridge Bay [2]. As suggested by the project name, the aim was to determine OTHR performance in the location of the earth's polar cap, near the magnetic pole.

Data gathered by Polar Fox II, along with a review of related auroral propagation studies, were reported in [3]. The frequent presence of auroral clutter led to design decisions during the US Air Force Over-the-Horizon Backscatter (OTH-B) radar acquisition program to restrict the OTHR field of view to the east, south, and west. For north-looking surveillance, a trip-wire line of microwave radars, called the North Warning System (NWS), was deployed along the 70th parallel in Canada in 1985. After the end of the Cold War in 1991, funding for the OTH-B program was cut, and the operation of the NWS was turned over to the Canadian Forces.

Since then, attention has shifted to systems that can continuously track targets within the entire North American airspace. Such a system would need to provide surveillance of an area of 50 million square kilometers, with a target altitude range of 0 to 30 kilometers. OTHR is an economical option for this task, as a single radar station can provide coverage of about 10 million square kilometers, and detect aircraft at all altitudes due to its "look down" vantage point.

In Canada, the auroral zone passes through the center of the country and is hard to avoid in any reasonable OTHR layout for airspace surveillance. Thus the approach of the effort described here is to tentatively accept the presence of auroral clutter and choose the lowest-cost locations for installing the radars. These locations would be in the south of the country, featuring northward-looking radars. In southern Canada, the supporting infrastructure is most readily available and construction complications are minimized. The proposed arrangement of OTHRs would thus be similar to the SuperDARN HF radar network [4]. Incidentally, the SuperDARN radars map the auroral zone ionospheric plasma convection by measuring the Doppler signatures of auroral radar clutter, and as such provide a large clutter database that can be used to cross-check data sets from Canadian OTHR systems.

In this memorandum, a description of the proposed signal processing is given in Section 2. It is shown in this section how Multiple-Input Multiple-Output (MIMO) techniques can be applied to provide clutter cancellation in both the transmit and receive portions of the radar system. A simplified covariance for the auroral clutter is used to derive analytic formulas for the improvement in signal-to-clutter ratio afforded by the processing. In Section 3, a new MIMO OTHR experiment is described, where auroral clutter data are collected and a basic illustration of clutter cancellation is shown. In Section 4 a conclusion is drawn and a proposal is made to upgrade the OTHR experimental testbed to larger power and aperture in order to verify the limits of the proposed techniques, and deploy transponders to test the techniques against realistic targets.

2 Signal processing

Auroral clutter arises due to Bragg scattering by plasma density irregularities in the auroral ionosphere. The density irregularities travel with the large-scale horizontal plasma convection in the auroral zone that is driven by the action of the solar wind on the magnetosphere [4]. We now discuss how this clutter is processed.

The description will proceed in two steps. First, we will discuss radar receive-side processing, which can be analyzed in terms of a simple clutter covariance matrix. Second, we will include transmit-side processing and show how it can be combined with receive-side processing. We will see that the effective processing gain is the product of the receive-side and transmit-side processing gains.

2.1 Radar receive component

The goal of the signal processing is to cancel the auroral clutter relative to a target signal. We first analyze the receive, or "multiple-output", component of the MIMO radar. For this analysis, let us consider an echo from a target consisting of a plane wave received by a fully sampled linear array of antenna elements spaced a distance $d = \lambda/2$ apart, where λ is the radar wavelength. The signal phase imparted by the physical layout of the linear array is captured by an array manifold vector $\mathbf{v}$:

$$\mathbf{v}^H = \left[\begin{array}{cccc} 1 & e^{-i\pi\sin\varphi} & e^{-2i\pi\sin\varphi} & \ldots \end{array} \right], \tag{1}$$

where H denotes conjugate transpose, and φ is the azimuthal angle of propagation of the plane wave with respect to the array boresight.

We then suppose that the plane wave target signal is corrupted by auroral clutter. The clutter is denoted by a random vector $\mathbf{n}$, where each element of $\mathbf{n}$ represents the clutter received at each sensor in the linear array. For analytic simplicity we assume that the clutter is centered on the array boresight, and the clutter autocorrelation perpendicular to the boresight direction has an exponential form:

$$R_n(z) = \sigma^2 e^{-|z|/L}, \tag{2}$$

where z is the lag along the array, L is the correlation length along the array, and σ^2 is the clutter variance. A first-principles derivation of the clutter autocorrelation function [5] shows that an exponential form underestimates the clutter correlation at small lags and overestimates at large lags, but the form is nevertheless useful to illustrate the signal processing principles. Defining the intersensor correlation coefficient as $\rho = \exp(-d/L)$, the sensor covariance matrix is

$$\mathbf{R}_n = \sigma^2 \begin{bmatrix} 1 & \rho & \rho^2 & & \\ \rho & 1 & \rho & & \\ \rho^2 & \rho & 1 & & \\ & & & \ddots & \end{bmatrix}, \tag{3}$$

where the variance of the clutter at all elements is taken to be σ^2.

Measurements taken by the elements of the receive array consist of the target vector plus the clutter, which we write as a vector $\mathbf{y}$:

$$\mathbf{y} = \mathbf{v}x + \mathbf{n}. \tag{4}$$

Here x is the complex amplitude of the plane wave signal, $\mathbf{v}x$ is the mapping of this plane wave signal onto the array elements, and $\mathbf{n}$ is the clutter observed at all array elements. We seek a linear estimator for x that consists of summing the measured signals according to a weighting function $\mathbf{w}$. The application of this estimator is described as

$$\hat{x} = \mathbf{w}^H \mathbf{y}. \tag{5}$$

One way to choose $\mathbf{w}$ is to minimize the random component of $\hat{x}$ under the constraint that the expected value of $\hat{x}$ is equal to x. This is referred to as the Minimum Variance Distortionless Response (MVDR) processor, and consists of the weights [6]

$$\mathbf{w}^H = \frac{\mathbf{v}^H \mathbf{R}_n^{-1}}{\mathbf{v}^H \mathbf{R}_n^{-1} \mathbf{v}}. \tag{6}$$

Of interest is the signal-to-clutter ratio (SCR) improvement of this processor. At the input, the signal is x and the clutter has variance σ^2. Therefore the input SCR is simply x^2/σ^2. At the output, the SCR is given by

$$\frac{x^2}{\sigma_{\hat{x}}^2} = \frac{x^2}{\langle (\hat{x} - x)(\hat{x} - x)^H \rangle}. \tag{7}$$

Combining the previous four equations, the output SCR can be found to be

$$\frac{x^2}{\sigma_{\hat{x}}^2} = x^2 \mathbf{v}^H \mathbf{R}_{\mathbf{n}}^{-1} \mathbf{v}. \tag{8}$$

The SCR improvement due to the processor is the ratio of the output SCR to the input SCR, which we denote as the array gain of the receive array [6]:

$$G_R = \sigma^2 \mathbf{v}^H \mathbf{R}_n^{-1} \mathbf{v}. \tag{9}$$

By multiplication with $\mathbf{R}_n$, one can prove that $\mathbf{R}_n^{-1}$ is given by

$$\mathbf{R}_n^{-1} = \frac{1}{\sigma^2(1-\rho^2)} \begin{bmatrix} 1 & -\rho & 0 & 0 & & & \\ -\rho & 1+\rho^2 & -\rho & 0 & & & \\ 0 & -\rho & 1+\rho^2 & -\rho & & & \\ 0 & 0 & -\rho & 1+\rho^2 & & & \\ & & & & \ddots & & \\ & & & & & 1+\rho^2 & -\rho \\ & & & & & -\rho & 1 \end{bmatrix}. \tag{10}$$

Using the notation $u = e^{i\pi \sin\varphi}$, the array gain is computed to be

$$G_R = \frac{N + (N-2)\rho^2 - (N-1)(\rho u + \rho u^{-1})}{1-\rho^2}, \tag{11}$$

where N is the number of sensors. G_R is large when $u \approx -1$ and $\rho \approx 1$. The condition $u \approx -1$ means that the target is well-separated from the clutter in azimuth angle, which can usually be satisfied if there are at least two radars looking at the scene from different directions (i.e., overlapping coverage). The condition $\rho \approx 1$ is equivalent to saying that the clutter should appear to originate from a narrow range of azimuth angles. Since the clutter arises from a large-scale convection pattern, the clutter will have different Doppler frequencies at different azimuth angles [4]. Thus, if necessary, Doppler processing can be used to confine the clutter to a narrow range of azimuth angles (a process referred to as "Doppler beam sharpening" in synthetic aperture radar applications). Under the conditions $u \approx -1$ and $\rho \approx 1$, the array gain of the MVDR processor is approximately

$$G_R \approx \frac{N(1+\rho)^2 - 2\rho(1+\rho)}{1-\rho^2} \tag{12}$$

$$= \frac{2(N-1)}{1-\rho}. \tag{13}$$

Clearly the clutter suppression becomes significant as the number of receive array elements N is made large, or as the intersensor clutter correlation coefficient ρ approaches unity.

2.2 Radar transmit component

We now consider the transmit, or "multiple-input", component of the MIMO radar. The multiple transmit channels are realized by transmitting orthogonal waveforms from each of M transmit elements and separating the individual transmitted signals received at each receive element using appropriate signal processing. The signals corresponding to each transmit channel can then be linearly combined to form an a posteriori transmit beam pattern.

The presence of M orthogonal waveforms adds complexity to the estimation problem. The observations at the receive array can now be written as

$$\mathbf{y} = \mathbf{v}_R \sum_{i=1}^{M} \upsilon_{Ti} x + \sum_{i=1}^{M} \mathbf{n}_i, \tag{14}$$

where $\mathbf{v}_R$ is the receive array manifold vector, υ_{Ti} is the ith element of the transmit array manifold vector, and $\mathbf{n}_i$ is the clutter related to emissions from the ith transmit element. The above model can be recast as follows:

$$\begin{aligned}
\mathbf{y}' = &\begin{bmatrix} \mathbf{v}_R \upsilon_{T1} \\ \mathbf{v}_R \upsilon_{T2} \\ \vdots \\ \mathbf{v}_R \upsilon_{TM} \end{bmatrix} x + \begin{bmatrix} \mathbf{n}_1 \\ \mathbf{n}_2 \\ \vdots \\ \mathbf{n}_M \end{bmatrix} && (15) \\
=&(\mathbf{v}_T \otimes \mathbf{v}_R) x + \mathbf{n}_C && (16) \\
\equiv&\mathbf{v}_C x + \mathbf{n}_C, && (17)
\end{aligned}$$

where $\otimes$ is the Kronecker product, $\mathbf{v}_C$ is a combined transmit-receive manifold vector, and $\mathbf{n}_C$ is a combined transmit-receive clutter vector whose covariance can be written as an $MN \times MN$ matrix given by

$$\mathbf{R}_{nC} = \mathbf{R}_{nT} \otimes \mathbf{R}_{nR}, \tag{18}$$

with $\mathbf{R}_{nT}$ being the covariance of the clutter across transmit elements and $\mathbf{R}_{nR}$ being the covariance of the clutter across receive elements (denoted simply $\mathbf{R}_n$ in the previous subsection).

Equation (17) is of the same form as Equation (4) and therefore an MVDR processor can be devised for the combined transmit-receive system. The array gain for the combined system is

$$\begin{aligned}
G_C &= \sigma_C^2 \mathbf{v}_C^H \mathbf{R}_{nC}^{-1} \mathbf{v}_C \\
&= \sigma_T^2 \sigma_R^2 (\mathbf{v}_T \otimes \mathbf{v}_R)^H (\mathbf{R}_{nT} \otimes \mathbf{R}_{nR})^{-1} (\mathbf{v}_T \otimes \mathbf{v}_R). && (19)
\end{aligned}$$

The inverse of a Kronecker product is the Kronecker product of the inverses, and the Hermitian conjugate of a Kronecker product is the Kronecker product of the Hermitian conjugates, thus

$$G_C = \sigma_T^2 \sigma_R^2 (\mathbf{v}_T^H \otimes \mathbf{v}_R^H)(\mathbf{R}_{nT}^{-1} \otimes \mathbf{R}_{nR}^{-1})(\mathbf{v}_T \otimes \mathbf{v}_R). \tag{20}$$

Recognizing the identity

$$(\mathbf{A} \otimes \mathbf{B})(\mathbf{C} \otimes \mathbf{D}) = \mathbf{AC} \otimes \mathbf{BD}, \tag{21}$$

leads to

$$\begin{aligned}
G_C &= \sigma_T^2 \sigma_R^2 (\mathbf{v}_T^H \mathbf{R}_{nT}^{-1} \otimes \mathbf{v}_R^H \mathbf{R}_{nR}^{-1})(\mathbf{v}_T \otimes \mathbf{v}_R) \\
&= (\sigma_T^2 \mathbf{v}_T^H \mathbf{R}_{nT}^{-1} \mathbf{v}_T) \otimes (\sigma_R^2 \mathbf{v}_R^H \mathbf{R}_{nR}^{-1} \mathbf{v}_R) \\
&= G_T G_R. \qquad (22)
\end{aligned}$$

Thus, the array gain of the combined system is simply equal to product of the array gains of the separate transmit and receive processors. For the combined processor it should be noted that under quasi-monostatic operation, the transmit and receive signal paths are similar, which would lead to a transmit array covariance similar to the receive array covariance. Thus the transmit processor improves performance by a factor of

$$G_T \approx \frac{2(M-1)}{1-\rho}. \qquad (23)$$

Generally the number of transmit channels M needs to be kept small, since the orthogonal waveforms must share a limited space in the radar range-Doppler ambiguity plane [7]. However, if $\rho \approx 1$ then the clutter cancellation on the transmit side can still be significant, resulting in good array gain on transmit.

While the MIMO principles have been illustrated above for beamforming in the azimuthal angular dimension φ, the same process could be used in the elevation dimension θ, since target signals for a given range gate generally arrive at a different elevation angle than those for the clutter. However, the elevation angle separation between target and clutter is generally small (i.e. $u \approx 1$), which severely limits the achievable array gain.

3 Experiment results

An experiment was set up in Ottawa, Ontario, Canada to perform some basic tests of MIMO signal processing for auroral OTHR clutter control.

3.1 Apparatus

A signal flowchart of the Ottawa system is shown in Figure 1. The orthogonal wave-

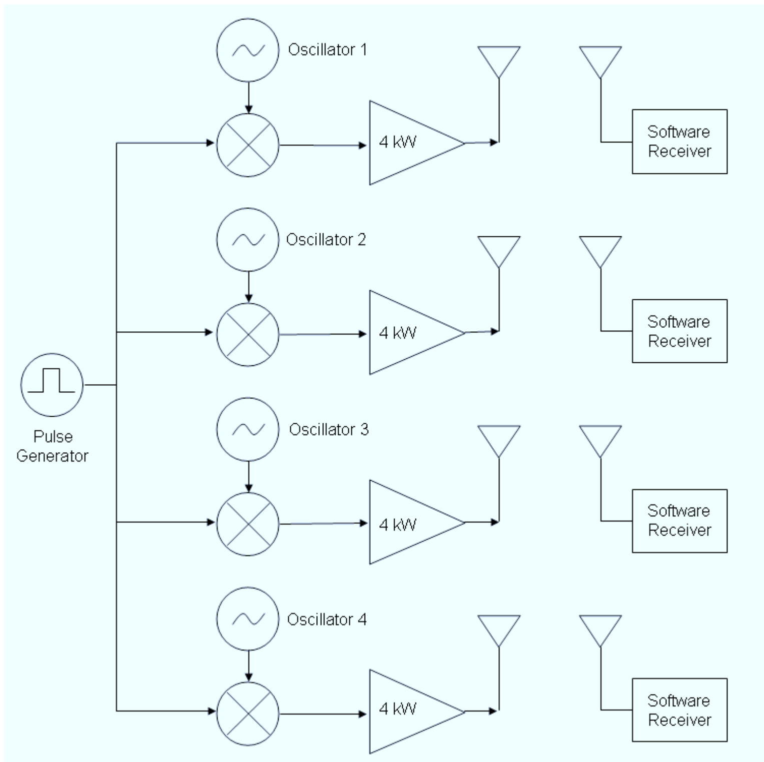

Figure 1: *Signal flowchart of experiment apparatus.*

form realization involves modulating a common waveform to M different carrier frequencies, each separated by a few Hz, sometimes referred to as slow-time MIMO [8]. Unlike familiar orthogonal waveform schemes, where waveforms are chosen to be separable by matched filter pulse compression, slow-time MIMO signals do not separate until after Doppler processing. In the Doppler-processed data, the waveforms appear Doppler-shifted from each other by their carrier frequency separations. Slow-time MIMO has the advantage that the transmit waveforms can be generated using low-cost signal generators rather than arbitrary waveform generators [8].

In the Ottawa experiment, a pulse generator creates a 5-ms duration pulse every 25 ms. The simple pulse waveform provides a range resolution of 750 km and the pulse repetition frequency of $f_p = 40$ Hz provides an unambiguous range of 3750 km. Thus the waveform provides five uncorrelated range gates, the first of which is eclipsed by the transmitted pulse. In the radar configuration of Figure 1, the pulse waveform is split four ways and each copy is modulated to a different carrier frequency. An example of a choice for a four-channel experiment would be carrier frequencies of $f_c + nf_p/4$, where f_c is the carrier frequency and $n \in \{0, 1, 2, 3\}$ is the channel number. Each of the 4 channels is then fed to a separate 4-kW amplifier and transmit antenna. This arrangement provides a peak power of 16 kW and an average power of 3.2 kW.

The transmit elements are wideband Beverage antennas. Each Beverage antenna consists of an end-fed horizontal copper wire 267 meters in length suspended 6 meters from the ground using five guyed poles equally spaced along the length of the antenna. The forward gain of each antenna at the carrier frequency of approximately 5 MHz is 4 dBi at 20 degrees elevation above the horizon. The Beverage antennas are parallel to each other and spaced 33.3 meters apart, providing a transmit aperture of 100 m.

On the receive side, a vertical monopole antenna is deployed 33.3 meters directly behind each transmit antenna, for a total of four monopole antennas, forming a 100-meter aperture. Each monopole is connected to a 14-bit direct-conversion digital receiver with a baseband data rate of 111.1 kHz, which writes IQ data to a 2-channel WAV-format computer file.

3.2 Experiment results: single-channel data

An experiment was performed in the evening of 5 Nov 2009 where two channels of the radar transmitter were used, running at carrier frequencies of 4.94150 MHz and 4.94152 MHz. This setup provided 20 Hz of separation between the signals in Doppler. On the receive side, the four receive channels were summed together to maximize gain in the boresight direction. Figure 2 shows a map of eastern Canada, with the location of the OTHR indicated as “Radar”. Also shown is the line of the radar boresight, which was aimed toward the magnetic pole to maximize visibility of the auroral zone. The radar range gates are denoted with numbers and tick lines on the boresight line. Finally, the curved contours show the trajectories of plasma convection during the experiment, obtained from the SuperDARN database at http://superdarn.jhuapl.edu/. Within the 750-km range and $\sim$1500-km azimuth extent of range gate 4, the line-of-sight plasma velocity varies between about 0 and 300 m/s, in a direction away from the radar. This corresponds to an expected Doppler shift between -10 and 0 Hz.

The radar data taken during the experiment are shown in Figure 3. Here we examine a single channel of data at 4.9415 MHz and interpret the clutter characteristics. The top panel in the figure shows the Doppler-processed data from range gate 4. The dwell time is 16 seconds, providing 0.06 Hz resolution. As predicted by inspection of the convection contours, the data show a broad auroral clutter echo spread between

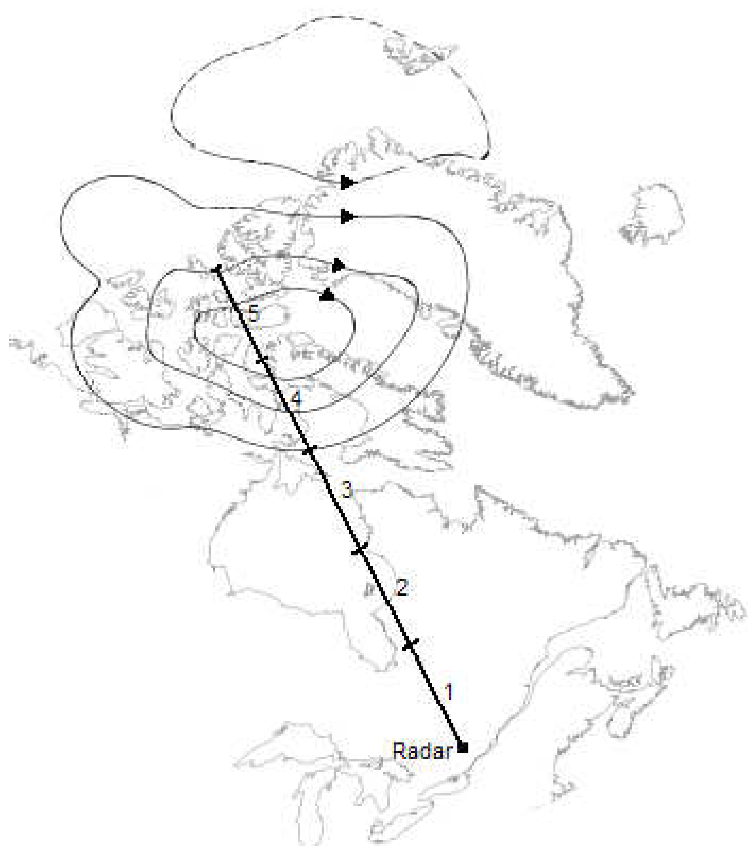

Figure 2: *Radar boresight, range gates, and trajectories of plasma convection.*

about -8 and 0 Hz in Doppler with about 10 dB clutter-to-noise ratio (CNR). The peak near 0 Hz is due to ground/ocean clutter.

For comparison, the bottom panel of Figure 3 shows the Doppler-processed radar data from range gate 3 of the radar. The broad auroral clutter echo is not present, and instead one sees narrow Bragg lines at a frequency of ± 0.23 Hz, corresponding to 30-m ocean waves in northern Hudson Bay that are Bragg-resonant with the 60-m radar wavelength.

3.3 Experiment results: dual-channel data

In Figure 4, we consider the data from two radar transmit channels, running at carrier frequencies 20 Hz apart. The two channels allow one to carry out transmit-side processing as described in Section 2.2, with the number of transmit channels set

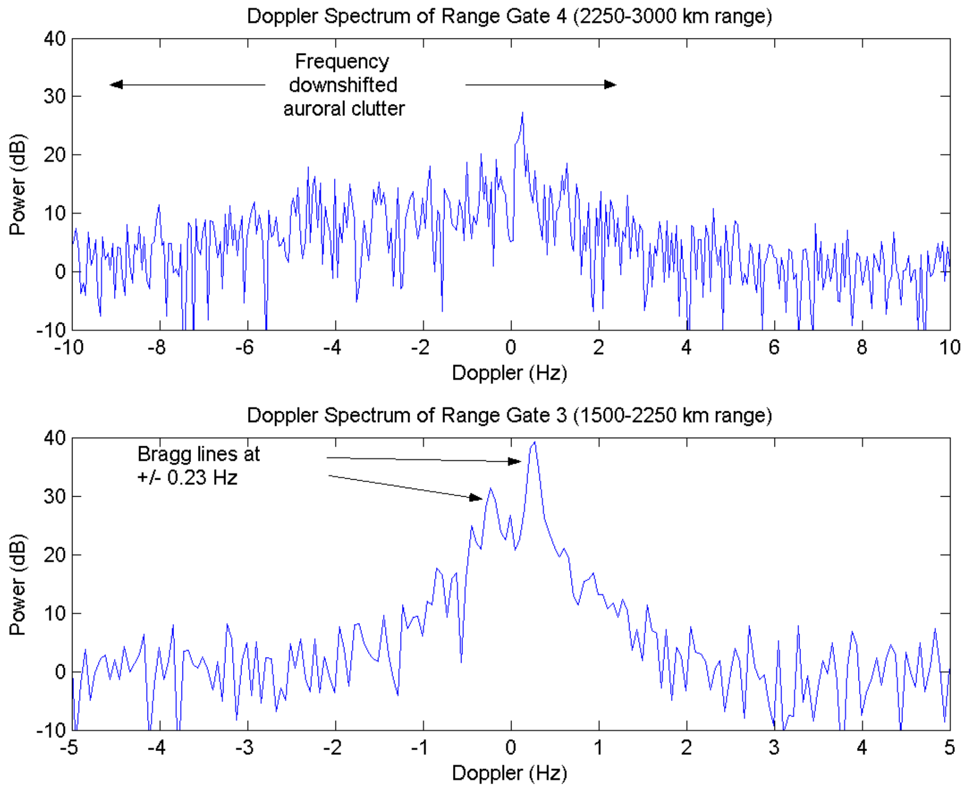

Figure 3: *Single-channel results, range gate 4 (top) and range gate 3 (bottom).*

at $M = 2$. After recording the data, the first step is to separate the two signals that are 20 Hz apart. The first transmit channel signal is extracted by mixing it to 0 Hz Doppler frequency and low-pass filtering the pulse sequence. The second transmit channel signal is extracted in the same manner. The separate channels are then Fourier-transformed. The auroral clutter echoes in the data are confined to roughly the range -8 to -1 Hz. The covariance of the two-channel clutter is thus estimated using Doppler frequency samples between -8 and -1 Hz.

An MVDR processor is then calculated. For this calculation, we suppose that there is a target located at a large angle to the clutter, such that $u \approx -1$, or equivalently, a manifold vector of $\mathbf{v}^H \approx [1 \quad -1]$.

Figure 4 shows the attempts to apply an MVDR processor to two different data sets. In each data set, the blue trace shows the data produced by a single transmit channel of the radar and the red trace shows the result of the MVDR processor applied to the dual-channel data. The data sets were taken on successive coherent integration dwells of the radar.

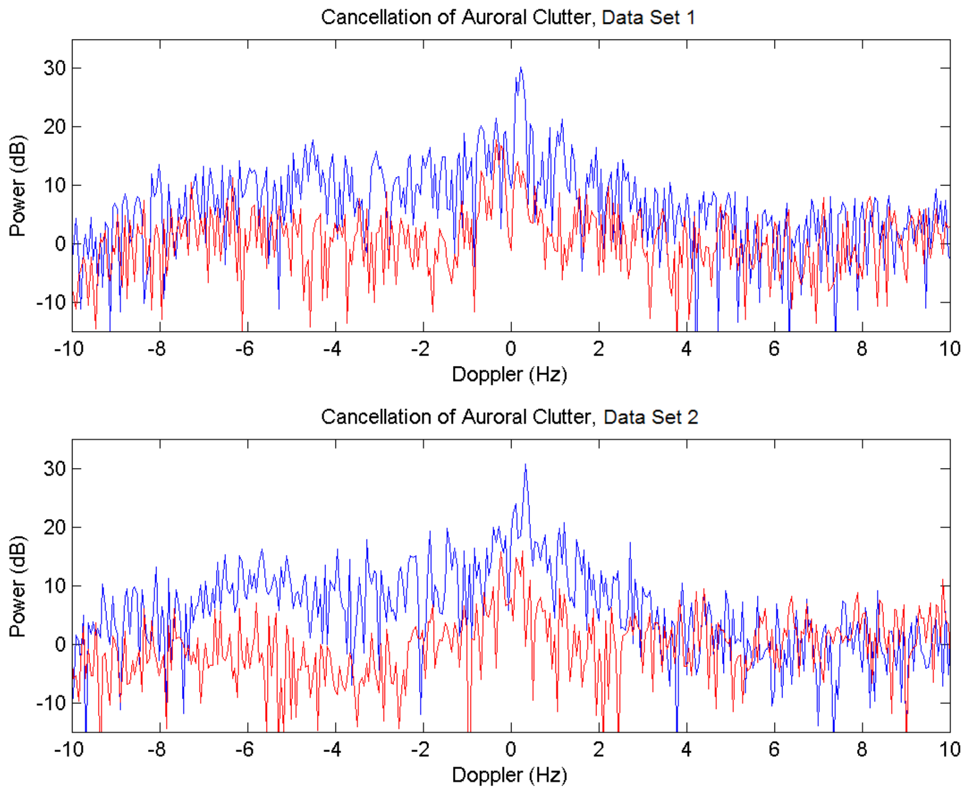

Figure 4: *Auroral clutter before cancellation (blue) and after cancellation using MVDR transmit processor (red).*

What is essentially happening is that this processor puts a null in the direction of the clutter. The results show that a single null can produce a 10-dB clutter suppression at all Doppler frequencies where the clutter is present. The ability of the transmit processor to cancel clutter beyond 10 dB is not possible to determine in this data set because the CNR of the clutter is only about 10 dB. Once the clutter reaches the white noise background level, further cancellation is minimal since the noise correlation is poor. Obviously, increased CNR would allow assessment of the full impact of the proposed signal processing, including both transmit and receive processing.

Another problem with the current configuration is that the three oscillators that control the Pulse Repetition Frequency (PRF), the transmit carrier frequencies, and the sampling frequency of the direct-conversion digital receiver, are not locked. This results in some trial and error in determining how to extract the two channels of data. For example, the lack of lock between the transmit carrier frequencies and the receiver sampling frequency means that a single random Doppler frequency offset is applied to both of the transmit channels. This offset requires one to translate the channels together in frequency until they appear to be symmetrically positioned around 0 Hz. This is currently done manually by inspection of the data. The two signals can then in principle be translated to 0 Hz for low-pass filtering by respectively up-translating and down-translating in Doppler frequency by a common frequency interval. However, the lack of lock between the PRF and the transmit carrier frequencies means that this common frequency interval is not exactly 10 Hz, which requires further inspection of the data.

The data presented in this subsection have been subject to the manual interventions described above. However, the interventions could be avoided by locking all three oscillators. The lock of the PRF and transmit carrier frequencies could be accomplished by triggering the pulse generator from a signal generator that is locked to the carrier frequency signal generators (which are locked to each other). The problem is that the PRF is not a radio frequency, so one would either need to synthesize the PRF from a difference of two radio frequencies, or count periods of a single radio frequency using a digital technique. An example of the latter would be the synthesis of a pulse by an arbitrary function generator whose sampling rate is clocked externally. The lock of the transmit frequencies and the receiver sampling frequency is somewhat easier to realize since the receivers used for this experiment can be modified to have the sampling frequency supplied by an external clock, which can be easily supplied by a signal generator locked to the carrier frequency signal generators. Implementing both locks would take some time but would considerably simplify the data analysis process.

4 Conclusions

This memorandum has briefly described methods to control auroral ionospheric clutter in a MIMO OTHR. Section 2 described the matter of MVDR processing of multiple transmit and receive channels. The level of clutter cancellation, expressed by the array gain, improves dramatically as the intersensor clutter spatial correlation coefficient approaches unity, with a somewhat less pronounced dependence on the number of transmit and receive channels. The number of transmit channels is constrained by the availability of space in the radar waveform ambiguity plane. The number of receive channels can be arbitrarily large assuming the simple exponential autocorrelation function for the clutter. However, more careful derivations of the correlation function [5] show that this simple model overestimates correlations at large lags along the array, which puts a maximum practical size on the receive array.

Section 3 presented some initial data and showed examples of auroral clutter cancellation using the proposed MIMO transmit processing scheme, in particular the use of multiple transmit channels that are orthogonal in the radar slow-time (pulse) dimension. While the clutter cancellation using two transmit channels was successful, the level of the clutter was only 10 dB above the noise floor. It is not clear whether the clutter is sufficiently correlated at higher CNR levels to permit complete cancellation. For example, the complete cancellation of 20-dB clutter with two transmit channels requires a 98% intersensor clutter correlation coefficient, which would almost certainly require narrowing the range of Doppler frequencies over which the sample covariance is computed. It remains to be shown experimentally whether such a narrowing is practical for realistic auroral plasma convection patterns. Furthermore, the lack of signal lock among the pulse repetition frequency, transmit carrier frequencies, and receive sampling frequency, complicates the analysis of the data through the requirement of manual correction of frequency offsets. These corrections can be avoided by using additional signal generators, locked to the carrier frequencies, that can clock the pulses and the receiver samples. Finally, the experiment could be retried with simultaneous multiple receive as well as transmit channels. Multiple receive channels are available in the system, but are currently hardwired to form a sum. The additional impact of adaptive receive processing on the clutter cancellation is not possible to determine due to the limited CNR of the auroral clutter that can be produced with the existing radar.

The major goal of further work should therefore be to significantly increase the CNR of the auroral clutter in the data to show the limit of the transmit nulling scheme, and further allow for exploration of receive-side processing. Specifically, it is proposed to increase the average transmit power by 10 dB (from 3.2 kW to 32 kW) by using a further four 4-kW amplifier units that are projected to be available in mid-2010, and then increasing the duty cycle of all eight 4-kW units to 100% by upgrading the amplifier DC power supplies. Further improvements could include another 10 dB of CNR through the installation of a 1-km aperture receive array about 15 km south of the transmit site, and the installation of a transponder north of the radar to provide a realistic target signal.

References

[1] Campbell, L. W., Katz, A. H., and Patton, D. E. (1972), Polar Fox II - experimental phase semi-annual technical report no. 1, (RADC-TR-72-21) Rome Air Development Center.

[2] Yool, S. (1973), Polar Cap III: Defence Research Board looks at over-the-horizon radar in Canada's Arctic, *Canadian Forces Sentinel*, 9.

[3] Elkins, T. J. (1980), A model for high frequency radar auroral clutter, (RADC-TR-80-122) Rome Air Development Center.

[4] Greenwald, R. A. et al. (1994), DARN/SuperDARN: A global view of the dynamics of high-latitude convection, *Space Science Reviews*, 71 (4), 761–796.

[5] Riddolls, R. J. (2008), Detection of aircraft by high frequency sky wave radar under auroral clutter-limited conditions, (DRDC Ottawa TM 2008-336) Defence R&D Canada–Ottawa.

[6] Van Trees, H. L. (2006), Optimum array processing, New York: Wiley, p. 445.

[7] Abramovich, Y. I. and Frazer, G. J. (2008), Bounds on the volume and height distributions for the MIMO radar ambiguity function, *IEEE Signal Processing Letters*, 15, 505–508.

[8] Mecca, V. F., Krolik, J. L., Robey, F. C., and Ramakrishnan, D. (2009), Slow-time MIMO spacetime adaptive processing, In J. Li and P. Stoica (Ed.), *MIMO radar signal processing*, pp. 283–318, New York: Wiley.

DOCUMENT CONTROL DATA

(Security classification of title, body of abstract and indexing annotation must be entered when the overall document is classified)

1. ORIGINATOR (the name and address of the organization preparing the document. Organizations for whom the document was prepared, e.g. Establishment sponsoring a contractor's report, or tasking agency, are entered in section 8.)

Defence R&D Canada - Ottawa
Ottawa, Ontario, K1A 0Z4

2. SECURITY CLASSIFICATION (overall security classification of the document, including special warning terms if applicable)

UNCLASSIFIED

3. TITLE (the complete document title as indicated on the title page. Its classification should be indicated by the appropriate abbreviation (S,C or U) in parentheses after the title.)

Initial results of HF sky wave radar experiments using MIMO methods to control auroral clutter (U)

4. AUTHORS (Last name, first name, middle initial)

Riddolls, Ryan J.

5. DATE OF PUBLICATION (month and year of publication of document)

January 2010

6a. NO. OF PAGES (total containing information. Include Annexes, Appendices, etc.)

28

6b. NO. OF REFS (total cited in document)

8

7. DESCRIPTIVE NOTES (the category of the document, e.g. technical report, technical note or memorandum. If appropriate, enter the type of report, e.g. interim, progress, summary, annual or final. Give the inclusive dates when a specific reporting period is covered.)

Technical Memorandum

8. SPONSORING ACTIVITY (the name of the department project office or laboratory sponsoring the research and development. Include the address.)

Defence R&D Canada - Ottawa
Ottawa, Ontario, K1A 0Z4

9a. PROJECT OR GRANT NO. (if appropriate, the applicable research and development project or grant number under which the document was written. Please specify whether project or grant)

Project 13mc06

9b. CONTRACT NO. (if appropriate, the applicable number under which the document was written)

10a. ORIGINATOR'S DOCUMENT NUMBER (the official document number by which the document is identified by the originating activity. This number must be unique to this document.)

DRDC Ottawa TM 2009-268

10b. OTHER DOCUMENT NOS. (Any other numbers which may be assigned this document either by the originator or by the sponsor)

11. DOCUMENT AVAILABILITY (any limitations on further dissemination of the document, other than those imposed by security classification)

(x) Unlimited distribution
( ) Distribution limited to defence departments and defence contractors; further distribution only as approved
( ) Distribution limited to defence departments and Canadian defence contractors; further distribution only as approved
( ) Distribution limited to government departments and agencies; further distribution only as approved
( ) Distribution limited to defence departments; further distribution only as approved
( ) Other (please specify):

12. DOCUMENT ANNOUNCEMENT (any limitation to the bibliographic announcement of this document. This will normally correspond to the Document Availability (11). However, where further distribution (beyond the audience specified in 11) is possible, a wider announcement audience may be selected.)

Unlimited

13. ABSTRACT (a brief and factual summary of the document. It may also appear elsewhere in the body of the document itself. It is highly desirable that the abstract of classified documents be unclassified. Each paragraph of the abstract shall begin with an indication of the security classification of the information in the paragraph (unless the document itself is unclassified) represented as (S), (C), or (U). It is not necessary to include here abstracts in both official languages unless the text is bilingual).

(U) High frequency Over-the-Horizon Radar (OTHR) provides an economical means to track noncooperative air targets over large expanses of land and ocean. However, early attempts to run OTHR in Canada in the 1970s were confounded by the presence of intense radar clutter originating in the auroral zone. Recent advances in Multiple-Input Multiple-Output (MIMO) OTHR technology, namely orthogonal waveform transmit arrays and fully sampled receive arrays, provide an opportunity to revisit the possibility of OTHR in Canada. An OTHR testbed has been built in Ottawa, Canada to determine the capabilities of the technology. The testbed consists of a MIMO OTHR with 4 transmit channels and 4 receive channels. Some preliminary data show that MIMO processing is effective in cancelling the clutter. It is then proposed to upgrade the testbed to a larger-scale system.

14. KEYWORDS, DESCRIPTORS or IDENTIFIERS (technically meaningful terms or short phrases that characterize a document and could be helpful in cataloguing the document. They should be selected so that no security classification is required. Identifiers such as equipment model designation, trade name, military project code name, geographic location may also be included. If possible keywords should be selected from a published thesaurus. e.g. Thesaurus of Engineering and Scientific Terms (TEST) and that thesaurus-identified. If it is not possible to select indexing terms which are Unclassified, the classification of each should be indicated as with the title.)

HIGH FREQUENCY
RADAR
OVER THE HORIZON
SKY WAVE
AURORA
RADIO
PROPAGATION
IONOSPHERE
PLASMA
IRREGULARITIES
CLUTTER
ANTENNA
ARRAY
MIMO

Defence R&D Canada

Canada's leader in Defence
and National Security
Science and Technology

R & D pour la défense Canada

Chef de file au Canada en matière
de science et de technologie pour
la défense et la sécurité nationale

DEFENCE R&D DÉFENSE

www.drdc-rddc.gc.ca